

Forward-electron-scattering study of the surface structure and phase transition on W(001)

Jaeyong Lee, Di-Jing Huang, and J. L. Erskine

Department of Physics, University of Texas at Austin, Austin, Texas 78712

(Received 12 December 1994)

Forward-electron-scattering measurements are used to investigate the surface structure and temperature-driven phase transition at the W(001) surface over the 100–770 K temperature range. Structural parameters obtained for the $c(2 \times 2)$ low-temperature phase, $T < 280$ K, are compatible with the Debe-King zig-zag chain model, but the temperature dependence of local surface structure deduced from forward-scattering measurements eliminates the possibility of a displacive transition to the (1×1) high-temperature phase as suggested by the interpretation of recent helium-atom-scattering experiments.

Early low-energy electron-diffraction (LEED) studies^{1–3} of W(001) established novel behavior of this surface. Below a critical temperature $T_c \approx 280$ K, the W(001) surface exhibits a low-temperature (LT) phase characterized by a $c(2 \times 2)$ symmetry LEED pattern; above T_c , a high-temperature (HT) phase forms which is characterized by a (1×1) LEED pattern. Numerous experiments^{1–15} have established that the LT $c(2 \times 2)$ to HT (1×1) transition is an intrinsic property of the clean surface, not the result of surface impurities. A corresponding phenomena has been observed on the (001) surface of Mo which like W is also a bcc metal.²

The structure of the LT phase has been studied by several experimental techniques including LEED,^{8,9} x-ray diffraction,^{11,12} ion-scattering,¹³ and core-level shifts.¹⁴ The basic (Debe-King) structure of the LT phase is shown in Fig. 1. The $c(2 \times 2)$ structure results from alternating lateral displacements of top layer atoms along $[\bar{1}10]$ directions characterized by the parameter Δ . This top-layer lateral displacement is accompanied by a relaxation of the top layer, characterized by d_{12} , and by a second-layer lateral displacement. The most recent LEED (Ref. 9) structural analysis of W(001) yields $\Delta = 0.21 \pm 0.04$ Å and $d_{12} = 1.485 \pm 0.025$ Å, which are in good agreement with the x-ray-diffraction^{11,12} results.

The structure of the (1×1) HT phase and the nature of

the phase transition remain controversial issues.^{3,4,7,15} Existing experimental studies of the reversible transition from the $c(2 \times 2)$ LT phase to the (1×1) HT phase have been interpreted as supporting either an order-disorder^{4,6,12,13} or displacive^{3,15} type transition. Extensive theoretical work^{16–22} has focused on the possible underlying driving forces leading to the LT structure and the statistical mechanics of the phase transition. Mechanisms considered include (short range) Jahn-Teller-like driven reconstruction, (long range) charge-density wave (CDW) and Fermi surface/surface-state models.²² Theoretical work^{17–22} generally favors an order-disorder model for the phase transition.

Figure 2 presents a schematic representation¹⁵ of the two basic phase-transition models being used to describe the observed symmetry change of the W(001) surface. At low temperature $T < T_c$, thermal energies are less than the barrier height in both cases, and a surface atom resides at one of the two potential minima. The site occupancy is correlated, leading to the Debe-King LT structural phase illustrated in Fig. 1. At elevated temperature, two possibilities arise depending on the local well depth in relation to the thermal energy. In the displacive transition, the surface-atom single-particle distribution function evolves to a single-peaked structure which cor-

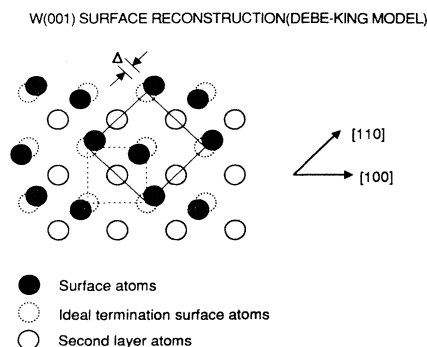


FIG. 1. Debe-King model for the LT $c(2 \times 2)$ W(001) surface reconstruction. The $c(2 \times 2)$ LEED pattern results from two orthogonal domains which exist in approximately equal population on real surfaces. The orthogonal domain corresponding to Fig. 1 is obtained by rotating the crystal 90° , yielding Δ along a $[\bar{1}10]$ direction.

SURFACE PHASE TRANSITION MODELS

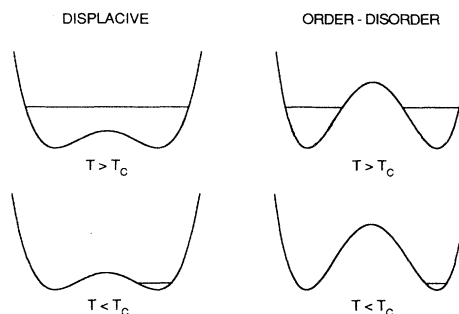


FIG. 2. Schematic representation of two phase-transition models for the LT to HT phase transition of W(001) (after Ref. 15). For $T < T_c$ in both models, a surface atom resides in one of the local minima of the potential well. For $T > T_c$, in the order-disorder model, the atom remains centered in one of the local minima, but the site-to-site correlation is lost (long-range order vanishes). In the displacive model, the thermal energy exceeds the well depth, and the atom resides in the center of the well.

responds to an ordered phase because the most probable location of the atom is the high-symmetry site. In the order-disorder transition, the thermal energy remains small compared to the local well depth and each atom continues to reside at one of the potential minima (away from the high-symmetry location). However, long-range correlation can be destroyed. In the specific case of W(001), this would result in the disappearance of the fractional beams of the $c(2\times 2)$ LEED pattern resulting in a (1×1) pattern.

The distinction between these two models becomes less clear when fluctuations are taken into account at temperatures near T_c . One way of viewing this is to note that the displacive transition will manifest order-disorder behavior near $T=T_c$. However, at temperatures sufficiently far from T_c , suitable experiments should be able to differentiate the two cases. The key issue is the temperature range over which the displacive model applies. Recent helium-atom-scattering studies¹⁵ of the structure and phonon dynamics of the W(001) surface over the temperature range from 200 to 1900 K have been interpreted as supporting the displacive phase-transition model for $T>450$ K. Temperature dependent shifts of half-order (LT phase) diffraction peaks are interpreted as being consistent with a $c(2\times 2)$ periodic lattice distortion based on the CDW mechanism. Corresponding shifts have not been observed in LEED or x-ray-diffraction experiments. Strong temperature dependence ($450\geq T\geq 220$ K) of a soft phonon mode and the appearance of new phonon modes ($T<220$ K) associated with the Brillouin-zone boundary of the $c(2\times 2)$ phase are also observed. These observations are used to argue that the overall phase transition associated with W(001) is of the displacive and not the order-disorder type.

Experimental evidence supporting the classification of the $c(2\times 2)$ LT to (1×1) HT transition as an order-disorder type is based on LEED,⁴ x-ray diffraction,¹² ion-scattering,¹³ and surface core-level shift studies.¹⁴ However, Ernst, Hulpke, and Toennies¹⁵ point out that all of these experiments, with the exception of the ion-scattering study, were performed below $T=400$ K, which is within the range where interpretation of the helium-atom-scattering experiments are also consistent with a disordered surface. At these lower temperatures, especially near T_c , both models can exhibit cluster-dominated short-range order with little or no static displacement characteristic of an order-disorder transition. In addition, Ernst, Hulpke, and Toennies reanalyzed the ion-scattering data assuming an ordered (1×1) high-temperature structure having an isotropic in-plane vibrational amplitude $\delta=0.13$ Å for surface atoms, but no static displacement from their bulk positions. They found that in the relevant temperature range (400–600 K), the ordered (1×1) HT model provides an equally satisfactory fit to ion-scattering data as was obtained using a disordered phase model. The conclusion reached by Ernst, Hulpke, and Toennies after considering all relevant experimental results is that the “overall classification of the temperature-induced phase transition as a displacive transition, which, in the vicinity of T_c , is dominated by fluctuations and a dynamical disorder

behavior, gives a coherent picture, thereby unifying the apparently contradicting experimental results.”

In this paper, we present experimental evidence which would appear to rule out any significant static (nonvibrational) displacement of surface atoms from their LT phase positions as a function of temperature between 100 and 770 K. This result clearly covers the temperature range above 450 K required to escape the short-range order regime in which a different both types of transitions will exhibit disorder, and directly supports an order-disorder model for the LT $c(2\times 2)$ to HT (1×1) structural transition.

Our results are based on forward electron scattering. Unlike diffraction experiments which are based on coherent scattering from a periodic lattice, forward scattering is sensitive primarily to local structure.²³ Fractional-order diffraction peaks associated with the $c(2\times 2)$ LT structure can vanish for two reasons: (1) static displacements occur above T_c , in which a different two-dimensional symmetry of the surface lattice is created (displacive transition); or (2) thermally induced loss of correlated static displacements occur over the coherence distance of the probing electron beam (order-disorder transition). Forward scattering is able to detect the presence or absence of surface-atom displacements even in cases where long-range correlation is lost. This renders it an ideal probe to investigate the surface phase transition on W(001).

Recent reviews²³ describe the forward-scattering technique for probing surface structure. The angular distribution of core-level photoelectrons are measured along selected crystallographic planes. Depending on the electron kinetic energy and other factors, the emitted intensity from second- and deeper-layer atoms in the crystal is either reduced or enhanced by forward scattering²³ or shadowing²⁴ by surface atoms. At relatively high kinetic energies (800–1000 eV), the effect is predominately an enhancement. A detailed description of our experimental methods which are used to probe surface structure based on forward scattering, including full multiple-scattering analysis of the scattering intensity to obtain structural parameters, is presented elsewhere.^{25,26} In this paper, we present sufficient discussion to establish the sensitivity of forward scattering to surface-atom displacements of W(001), and to document the compatibility of our W(001) surface structural parameters (which in the present discussion are obtained from simple geometrical models) with existing experiments, specifically the recent LEED (Ref. 9) and x-ray-diffraction¹¹ results. This provides the basis for interpretation of our temperature-dependent forward-scattering data in terms of an order-disorder model.

Figure 3 displays three pairs of forward-scattering angular distributions for W(001) in the $[001]$ - $[110]$ plane corresponding to the direction of maximum surface-atom displacement. Each pair of spectra represent a different kinetic energy. Using Mg $K\alpha$ radiation, the kinetic energies are: $(W4d_{5/2})$ 1006 eV, $(W4d_{3/2})$ 992 eV, and $(W4p_{3/2})$ 825 eV. The primary peaks ($A-D$) which are observed at specific angles for the two higher electron kinetic energies have a structural origin. Peaks which ex-

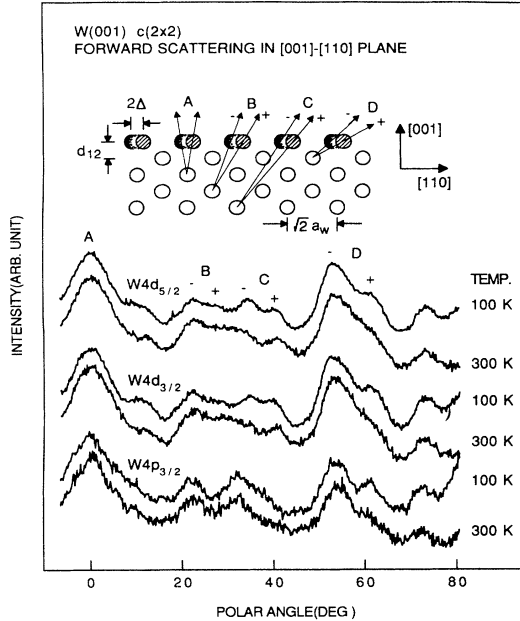


FIG. 3. Temperature and electron kinetic-energy dependence of forward-scattering angular distributions from W(001) in the [001]-[110] plane. The inset illustrates the scattering plane crystal structure and the origin of peaks *A*, *B*, *C*, and *D*. Displaced surface atoms are shown shaded.

hibit sensitivity to electron energies, as is apparent in the lower energy ($W4p_{3/2}$) spectra, generally contain contributions from multiple scattering. The peaks labeled B_{\pm} , C_{\pm} , and D_{\pm} are identified as resulting from the scattering process labeled correspondingly in the crystal model displayed as an inset.

Figure 4 displays corresponding temperature-dependent forward-scattering angular distributions for W(001) in the [001]-[100] plane. These spectra do not exhibit the splitting apparent in Fig. 3. In this case, the surface-atom displacements are at $\pm 45^\circ$ with respect to the scattering plane, and the scattering is much less sensitive to the lateral displacements.²⁶ Thus forward-scattering spectra displayed in Figs. 3 and 4 manifest direct experimental evidence of the Debe-King model.

An estimate of the structural parameters Δ and d_{12} can be obtained from the forward-scattering angular distributions of Figs. 3 and 4. It is a straightforward exercise to show, using the Debe-King model (based on a simple geometrical interpretation of the forward-scattering peaks in which maximum scattering occurs along inter-nuclear axes and neglecting second-layer reconstruction^{9,11}), that, for peak *C* in Fig. 4,

$$d_{12} = a_w (\cot \theta_c - 0.5) \text{ \AA}, \quad (1)$$

where $a_w = 3.16 \text{ \AA}$, the W lattice constant; and that, for the pair of peaks D_{\pm} in Fig. 3,

$$\tan \theta_{D-} = (2.434 - \Delta) / d_{12}, \quad (2)$$

$$\tan \theta_{D+} = (2.434 + \Delta) / d_{12}. \quad (3)$$

By curve fitting the peak at $\theta = 0$ (for accurate reference to the crystallographic [001] axis), the single peak *C* in Fig. 4 and the multiple-component peak D_{\pm} of the W_{4d} angular distributions in Fig. 3, we obtain accurate values

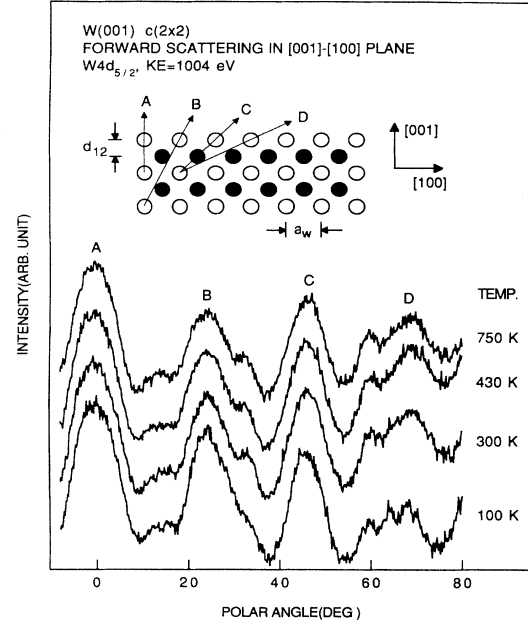


FIG. 4. Forward-scattering angular dependence from W(001) in the [001]-[100] plane in which surface-atom displacements are predominately perpendicular to the scattering plane. The inset illustrates the scattering plane crystal structure and the origin of peaks *A*, *B*, *C*, and *D*.

for θ_c , θ_{D+} and θ_{D-} which are used to solve Eqs. (1)–(3) for d_{12} and Δ . We obtain $d_{12} = 1.43 \text{ \AA}$ and $\Delta = 0.39 \text{ \AA}$. Peaks C_{\pm} in the W_{4d} angular distributions are insensitive to d_{12} because of the smaller polar angle, but can be used to obtain an independent value for $\Delta = 0.40 \text{ \AA}$. While the magnitude of Δ estimated from forward scattering is significantly larger than that established from LEED and x-ray diffraction, it is significantly smaller than the practical limit imposed by steric considerations ($\Delta_{\max} \sim 0.6 \text{ \AA}$) when zig-zag surface atoms are in contact with r approximately equal to half the bulk atom nearest-neighbor separation.

Two points regarding the asymmetric double-peak character of peaks *B*, *C*, and *D* in Fig. 3 must be addressed later in relation to curve fitting and temperature-dependent broadening of temperature-dependent data. There are three components to these peaks; two result from scattering by displaced surface atoms (inset), and the third results from scattering of electrons emitted from third-layer atoms by undisplaced second-layer atoms. It is clear that an accurate structure determination based on this method will require careful attention to layer dependencies and multiple-scattering effects.²⁶ However, for our present purpose, the above discussion, including the estimated structural parameters stated above, represents adequate demonstration of the structural sensitivity of the method when applied to the LT reconstruction of W(001). It is interesting to note that for forward scattering $\Delta k = 0$, and Debye-Waller effects vanish. However, peak broadening resulting from increased vibrational amplitudes is apparent in the angular distributions obtained at higher temperatures.

Figure 5 displays typical results of curve-fitting temperature-dependent forward-scattering angular distri-

butions in the [001]-[110] plane for $4d_{5/2}$ W core-level emission. Similar curve fitting was carried out for numerous temperature-dependent spectra including those shown in Fig. 3; the results are compiled as plots of temperature-dependent values of Δ and d_{12} in Fig. 5. Two constraints were imposed: (1) the weights of peaks *a* and *b* were assumed to be equal, and (2) the location of peak *c* was fixed at 55° based on the bulk W lattice parameter. The result of curve fitting over a dozen spectra to obtain θ_{D+} and θ_{D-} and solving for d_{12} and Δ is that essentially no variation of these parameters can be detected as a function of temperature from 100 to 770 K. Corresponding analysis of temperature-dependent forward scattering angular distributions in the [001]-[100] plane (Fig. 4) yielded the same conclusion. The absolute accuracy of our determination of d_{12} and Δ is not stated here because a realistic assessment must be based on a thorough analysis of multiple-scattering effects which will be reported separately.²⁶ We can state the precision of our determination of d_{12} and Δ , which can be judged from the repeatability of the experimental determinations of d_{12} and Δ . This is more relevant to our present discussion, which focuses primarily on a search for temperature-dependent changes in the thermally averaged surface-atomic displacements which could be interpreted as an indication of a displacive transition. The precision of our angle determination including curve fitting and mechanical precision of the rotation platform used in our experiments is estimated to be $\pm 0.3^\circ$ which translates into a precision of $\pm 0.03 \text{ \AA}$ for the parameters d_{12} and Δ . Within this precision, we interpret our results as indicating that no measurable static displacements of the Debe-King reconstruction occurs over the temperature range 100–770 K, suggesting that the W(001) LT $c(2 \times 2)$ to HT (1×1) transition is best characterized as an order-disorder transition over this temperature range.

In summary, forward-scattering angular distributions directly confirm the LT Debe-King reconstruction of W(001), but appear to yield a surface displacement parameter Δ significantly larger than the value established by LEED and x-ray diffraction. Multiple-scattering cal-

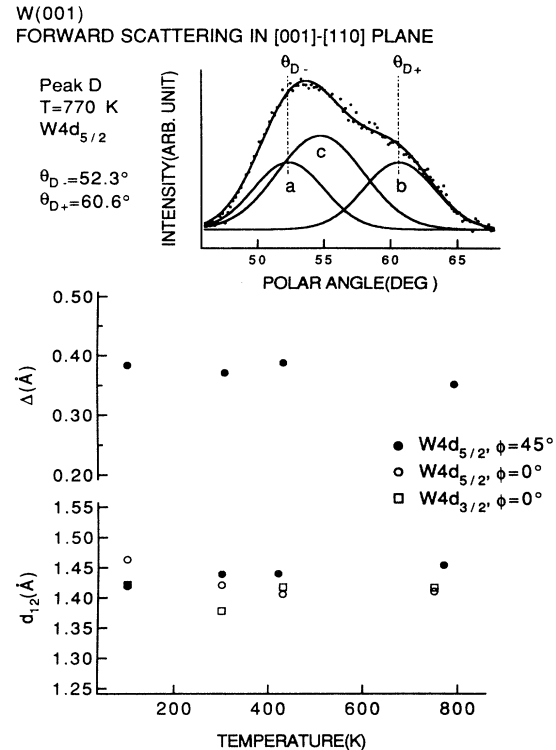


FIG. 5. Typical curve-fitting result for peak D_{\pm} which determines $\theta_{\Delta+}$ and $\theta_{\Delta-}$. Lower panels, plot of Δ and d_{12} vs temperature obtained from forward scattering. Note that for the $\phi=0^\circ$ configuration [100] plane, only d_{12} can be determined.

culations leading to an accurate error analysis of the forward-scattering result or an independent direct structural measurement of Δ by scanning tunneling microscopy (STM) may resolve this discrepancy. Temperature-dependent studies of the surface structure reveal essentially no departure of local structure from the Debe-King model up to 770° K , confirming the order-disorder character of the LT \rightarrow HT transition.

This work was supported by NSF DMR 9303091 and the Robert A. Welch Foundation, Grant No. F-1015.

¹K. Yonehara and L. D. Schmidt, *Surf. Sci.* **25**, 238 (1971).

²T. E. Felter *et al.*, *Phys. Rev. Lett.* **38**, 1138 (1977).

³M. K. Debe and D. A. King, *J. Phys. C* **10**, L303 (1977); *Phys. Rev. Lett.* **39**, 708 (1977); *Surf. Sci.* **81**, 193 (1979).

⁴R. A. Barker and P. J. Estrup, *J. Chem. Phys.* **74**, 1442 (1981).

⁵M. K. Debe and D. A. King, *J. Phys. C* **15**, 2257 (1982).

⁶J. F. Wendelken and G. C. Wang, *Phys. Rev. B* **32**, 7542 (1985); *Surf. Sci.* **140**, 425 (1984).

⁷D. L. Roelofs and J. F. Wendelken, *Phys. Rev. B* **34**, 3319 (1986).

⁸J. A. Walker *et al.*, *Surf. Sci.* **104**, 405 (1981).

⁹G. Schmidt *et al.*, *Surf. Sci.* **271**, 416 (1992).

¹⁰I. Stensgaard *et al.*, *Phys. Rev. Lett.* **42**, 247 (1979); *Surf. Sci.* **87**, 410 (1979).

¹¹M. S. Altman *et al.*, *Phys. Rev. B* **38**, 5211 (1988).

¹²I. K. Robinson *et al.*, *Phys. Rev. Lett.* **62**, 1294 (1989).

¹³I. Stensgaard *et al.*, *Phys. Rev. B* **39**, 897 (1989).

¹⁴J. Jupille *et al.*, *Phys. Rev. B* **39**, 6871 (1989).

¹⁵H.-J. Ernst *et al.*, *Phys. Rev. B* **46**, 16081 (1992).

¹⁶C. L. Fu *et al.*, *Phys. Rev. Lett.* **54**, 2261 (1985); C. L. Fu and A. J. Freeman, *ibid.* **57**, 3292 (1986); *Phys. Rev. B* **37**, 2685 (1988).

¹⁷R. Yu *et al.*, *Phys. Rev. B* **45**, 8671 (1992).

¹⁸A. Fasolino and E. Tosatti, *Phys. Rev. B* **35**, 4264 (1987).

¹⁹C. Z. Wang *et al.*, *Europhys. Lett.* **6**, 43 (1988).

²⁰L. D. Roelofs, *Surf. Sci.* **178**, 396 (1986); *Phys. Rev. B* **34**, 3337 (1986).

²¹L. D. Roelofs *et al.*, *Phys. Rev. B* **40**, 9147 (1989).

²²K. E. Smith *et al.*, *Phys. Rev. B* **42**, 5385 (1990).

²³W. F. Egelhoff, Jr., *Crit. Rev. Solid State Mater. Sci.* **16**, 213 (1990); H. C. Poon and S. Y. Tong, *Phys. Rev. B* **30**, 6211 (1984); C. S. Fadley, *Prog. Surf. Sci.* **16**, 275 (1984); S. A. Chambers, *Adv. Phys.* **40**, 357 (1991).

²⁴J. J. Barton and L. J. Terminello, *Phys. Rev. B* **46**, 13548 (1992).

²⁵B. Kim *et al.*, *Phys. Rev. B* **48**, 4735 (1993).

²⁶J. Lee, D.-J. Huang, J. L. Erskine, W. N. Mei, and C. M. Wei (unpublished).